NASA Technical Memorandum 101352

Leakage Predictions for Rayleigh-Step, Helium-Purge Seals

Margaret P. Proctor
Lewis Research Center
Cleveland, Ohio

December 1988

NASA

LEAKAGE PREDICTIONS FOR RAYLEIGH-STEP, HELIUM-PURGE SEALS

Margaret P. Proctor
National Aeronautics and Space Administration
Lewis Research Center
Cleveland, Ohio 44135

SUMMARY

Rayleigh-step, helium-purge, annular shaft seals, studied for use in liquid oxygen turbopumps, generate a hydrodynamic force that enables the seal to follow shaft perturbations. Hence, smaller clearances can be used to reduce the seal leakage. FLOWCAL, a computer code developed by Mechanical Technology Incorporated, predicts gas flow rate through an annular seal with an axial pressure gradient. Analysis of a 50-mm Rayleigh-step, helium-purge, annular seal showed the flow rate increased with increased axial pressure gradient, downstream pressure, and eccentricity ratio. Increased inlet temperature reduced the leakage. Predictions made at maximum and minimum clearances (due to centrifugal and thermal growths, machining tolerances and ±2 percent uncertainty in the clearance measurement) placed wide boundaries on expected flow rates. The widest boundaries were set by thermal growth conditions. Predicted flow rates for a 50-mm Rayleigh-step, helium-purge, annular seal underestimated measured flow rates by three to seven times. However, the analysis did accurately predict flow rates for choked gas flow through annular seals when compared to flow rates measured in two other independent studies. Possible causes for the discrepancy found between measured and predicted flow rates are discussed. Further testing is recommended.

E-4379

INTRODUCTION

Rayleigh-step, helium-purge, annular seals are being studied for use in liquid oxygen turbopumps. The hydrodynamic force generated by the Rayleigh-steps increases the seal stiffness and allows it to closely follow shaft perturbations. Besides reducing the likelihood of a damaging rub, this seal capability allows the designer to use tighter seal clearances, which result in reduced leakage.

Under a contract directed by NASA Lewis Research Center (NAS3-23260), Mechanical Technology Incorporated (MTI) developed two analytical computer codes to assist in designing Rayleigh-step, annular seals. MTI also designed and fabricated test seals for 20-mm and 50-mm shafts and compiled a small amount of experimental data for the 50-mm shaft seal.

Presently, an experimental study is underway at NASA Lewis to complete testing of the Rayleigh-step, helium-purge, annular seals and to validate the computer codes. One of the codes developed by MTI, RASTEPCO, calculates the Rayleigh-step performance and the pressure distribution on the pads. Discussion of this code, however, is beyond the scope of this paper. The other code, FLOWCAL, predicts the leakage rate across the sealing dam. Predicted flow rates generated with FLOWCAL underestimated the measured flow rates for the 50-mm Rayleigh-step, helium-purge, annular seal by three to seven times. Hence, the aim of this paper is to discuss the validity of using FLOWCAL to predict flow rates for this seal design. The design of the Rayleigh-step annular seal that was tested, and the analysis that was used in FLOWCAL are presented. Flow rate predictions, to illustrate the effects various test and

manufacturing parameters have on the leakage rate, and comparisons of predicted and measured flow rates follow. Possible causes for the discrepancies are discussed as well as a plan of action to completely validate the use of FLOWCAL for this seal design.

SYMBOLS

A	annular area, $in.^2$
C	concentric radial clearance, in.
C_D	discharge coefficient
D	shaft diameter, in.
e	eccentricity, in.
g_c	386 lbm-in./lbf-sec^2
ℓ	seal dam length, in.
$\dot{m}$	mass flow rate, lbm/sec
$\bar{\dot{m}}$	$\dot{m}/\dot{m}_o$
$\dot{m}_o$	$P_s^2 C^2 (1 + 3/2\ \epsilon^2) A/(24\ RT_s\ \mu\ell)$
P	pressure, psia
P_a	downstream pressure, psia
$\bar{P}_a$	P_a/P_o, normalized downstream pressure
P_c	Pressure at which choked flow occurs, psia
$\bar{P}_c$	P_c/P_o, normalized downstream pressure at which choked flow occurs
P_d	P_s-P_a, pressure drop across seal, psid
P_i	intermediate pressure, psia
$\bar{P}_i$	P_i/P_o, normalized intermediate pressure
P_o	reference pressure, psia
P_s	inlet stream pressure, psia
R	gas constant, lbf-in./lbm-°R
Re	Reynolds number

T temperature, °R

T_i intermediate temperature, °R

$\bar{T}_i$ T_i/T_s, normalized intermediate temperature

T_s upstream or inlet temperature, °R

v velocity, in./sec

x distance, in.

β $2RT_s (\dot{m}_o/AP_s)^2/g_c$

γ specific heat ratio

ϵ e/c, eccentricity ratio

μ fluid absolute viscosity, lbf-sec/in.^{2}

ρ fluid density, lbm/in.^{3}

RAYLEIGH-STEP ANNULAR SEAL

Figure 1 is a photograph of the 50-mm Rayleigh-step shaft seals and runner that were tested. Each ring is made of Purebon P5N carbon graphite to minimize the mass moment of inertia of the seal, thereby improving the seal's capability to track shaft perturbations. Four capacitance probes (two diametrically opposed pairs) were embedded in the seal ring to measure the seal clearance directly. The pairs were 70° apart to facilitate eccentricity measurements. Seal dimensions are presented in figure 2, which shows the inner surface of the seal ring. The pocket depth of 0.001 inches is sufficient to generate a hydrodynamic force during shaft rotation. The rotating shaft pulls fluid from the axial grooves into the pockets and over the lands, creating a pump-like effect, or the hydrodynamic force. The schematic in figure 3 shows how the seal pairs are installed. A wavy washer separates the two seal rings and holds them against the housing. To ensure the seals' ability to respond to shaft perturbations, the frictional force between the seal rings and the housing is minimized by a small axial lip (and hence small contact area between the seal ring and housing) radially positioned to nearly balance the opposing axial pressure forces.

FLOWCAL

Theory

FLOWCAL calculates either isothermal or adiabatic gas flow rates through an annular clearance with an axial pressure gradient. Eccentricity and inlet inertial effects are accounted for. The seal is divided into two regions; an inlet region where the flow is strictly inertial and a film region where viscous forces dominate (see fig. 4). At the inlet, the flow rate is computed as in a flow nozzle by the following equation:

$$\dot{m} = C_D A \left(\frac{2\gamma}{\gamma - 1}\right)^{1/2} P_s \left(\frac{g_c}{RT_s}\right)^{1/2} \left(1 - \bar{P}_i^{(\gamma-1)/\gamma}\right)^{1/2} \bar{P}_i^{1/\gamma} \tag{1}$$

The critical pressure for choked flow is

$$\bar{P}_c = \left(\frac{2}{\gamma + 1}\right)^{\gamma/(\gamma-1)} \tag{2}$$

If the normalized pressure downstream of the inlet, $\bar{P}_i$, becomes less than the critical presure $\bar{P}_c$, then $\bar{P}_i$ is set equal to $\bar{P}_c$ and the mass flow rate becomes

$$\dot{m} = C_D A \left(\frac{g_c \gamma}{RT_s}\right)^{1/2} P_s \left(\frac{2}{\gamma + 1}\right)^{(\gamma+1)/2(\gamma-1)} \tag{3}$$

In the film region, the following equations apply:

$$\int \left(\frac{dP}{dx} + \frac{1}{gc} \rho v \frac{dv}{dx}\right) dx = \frac{-12\ \mu \ell}{C^2\left(1 + \frac{3}{2}\epsilon^2\right)} v \tag{4}$$

$$\dot{m} = \rho v A, \qquad \rho = \frac{P}{RT} \tag{5}$$

Combining equations (4) and (5) and normalizing yields

$$\frac{2\gamma}{1 + \gamma} \frac{\bar{P}_i^{(\gamma-1)/\gamma}}{\bar{T}_i} \left(\bar{P}_i^{(1+\gamma)/\gamma} - \bar{P}_a^{(1+\gamma)/\gamma}\right) - \frac{\beta \bar{\dot{m}}^2}{\gamma} \ln\left(\frac{\bar{P}_i}{\bar{P}_a}\right) = \bar{\dot{m}} \tag{6}$$

The critical pressure at which choking will occur is found by differentiating with respect to $\bar{P}_a$, setting $d\bar{\dot{m}}/d\bar{P}_a = 0$, and solving for $\bar{P}_a$. This value of $\bar{P}_a$ is the critical pressure, $\bar{P}_c$, where

$$\bar{P}_c = \frac{\beta \bar{\dot{m}}^2}{2\gamma} \frac{\bar{T}_i}{\bar{P}_i^{(\gamma-1)/\gamma}}^{\gamma/(1+\gamma)} \tag{7}$$

Again, if $\bar{P}_a < \bar{P}_c$, then set $\bar{P}_a = \bar{P}_c$. If the flow is isothermal, then $\gamma = 1$ in the film region equation.

To compute the flow rate through the seal, a value is estimated for the intermediate pressure $\bar{P}_i$ immediately downstream of the inlet. This value is used to calculate the mass flow rates in both the inlet and film regions. Upon the comparison of the flow rates, a new value for $\bar{P}_i$ is selected and the process repeated until the difference between the flow rates is within a given tolerance or the maximum number of iterations permitted has been reached. The iteration process is an accelerated Newton-Raphson method.

The following major assumptions are made in this analysis:

(1) The annular clearance is small compared to the shaft radius.
(2) The gas is an ideal gas.
(3) The viscosity and specific heat ratio of the gas remain constant.

Input and Output

Some of the input required for FLOWCAL is illustrated in figure 4. The fluid conditions and properties needed are the upstream pressure and temperature, the downstream pressure, viscosity, molecular weight and specific heat ratio. Geometrical input required are the shaft diameter, seal length, radial clearance, eccentricity ratio, and discharge coefficient. Normally the value of the discharge coefficient is between 0.6 and 1.0. The program has the option to calculate adiabatic or isothermal flow. The program output are film temperature, pressure and Reynolds number; choked flow pressure; flow rate; and flow error. The flow error is the difference between the flow rates calculated from the inlet region equation and the film region equation.

ANALYTICAL RESULTS AND DISCUSSION

Parametric predictions were made to illustrate how the flow rate is affected by operating conditions and to bound the predicted flow rate range by machining tolerances and reasonable levels of measurement uncertainty. Predictions were made for both the 50-mm and 20-mm diam shaft sizes. However, only results for the 50-mm diam shaft are presented here. Predictions for the 20-mm diam shaft may be found in the appendix. The baseline geometry and operating conditions used in making the flow rate predictions are shown in table I. These conditions are used in all cases except where otherwise specified on the figures.

The baseline cases for adiabatic and isothermal flows are shown in figure 5. The volumetric flow rate (leakage rate) in standard cubic feet per minute (SCFM), which is directly proportional to mass flow rate, is plotted as a function of the pressure drop across the seal P_d. As expected, the flow rate increases with an increase in P_d. Leakage rates for adiabatic flow are greater than for isothermal flow and the difference increases with increased P_d.

The effect of the downstream pressure on flow rate is shown in figure 6. Predictions were made for three downstream pressures: 14.7, 45.0, and 75.0 psia. Note that the upstream pressure is the sum of the downstream pressure and the pressure drop across the seal. Flow rates are greater for the

higher downstream pressures because the fluid density is greater. At a pressure drop across the seal of 100 psid or more, the slopes of all three curves are nearly equal.

Figure 7 shows the leakage rate as a function of inlet stream temperature for P_d equal to 40.0 psid. The correct viscosity for each inlet temperature was used. The flow rate decreases as the inlet temperature increases because the fluid density is inversely proportional to temperature as stated in the ideal gas law. Superimposed on the linear effect of density change is the nonlinear effect of viscosity, which increases with temperature and further reduces the leakage rate.

Figure 8 is a plot of predicted flow rate with respect to eccentricity ratio ε. The leakage rate is only slightly affected by an increase in eccentricity ratio as long as $\varepsilon \leq 0.2$. For $\varepsilon > 0.2$ the flow rate is dramatically increased. This result is consistent with the experimentally verified analysis done by Tao and Donovan (ref. 1). The ratio of the fully eccentric flow rate to the concentric flow rate for the pressure drop across the seal of 5.0 and 115.0 psid are 2.466 and 1.564, respectively. Calculation of the Reynolds number shows that at P_d = 5.0 psid the flow is laminar (Re = 33.5) and that at P_d = 115.0 psid the flow is turbulent (Re = 4415). In reference 1, analysis and experimental data show that the fully eccentric to concentric flow rate ratio should be approximately 2.5 for laminar flow and between 1.2 and 1.4 for turbulent flow. This supports the predictions made with FLOWCAL.

In an effort to bound the range of flow rates to be measured, predictions were made for the extreme cases of centrifugal and thermal growths, machining tolerances, and a ±2 percent uncertainty in the clearance measurements. All of these items change the range of clearances at which the seal operates. Since the flow rate is a function of the clearance cubed, minor changes in the clearance can have significant results.

The amount of centrifugal growth of the 50-mm diam runner for the Rayleigh-step, helium-purge seal may be found in reference 2. Predicted flow rates for five different shaft speeds are shown in figure 9. As expected, flow rates are lower for the higher shaft speeds because the seal clearance has been reduced by centrifugal growth of the shaft.

In order to band the range of flow rates due to thermal growth effects of the seal and runner, the two extreme cases were considered. The maximum clearance due to the thermal effects is obtained when the shaft is at the temperature of liquid nitrogen (-320 °F) and the seal ring is at the temperature of ambient helium (70 °F). (Liquid nitrogen hydrostatic bearings are used in the seal tester to support the shaft; hence the shaft gets extremely cold.) The minimum clearance occurs when the shaft and seal ring both operate at ambient (70 °F) conditions. The flow rates predicted for these two conditions are shown in figure 10.

Another way to bound the flow rates is to make predictions based on the machine tolerances allowed in the fabrication of the shaft runner and seal ring. This is illustrated in figure 11. At a 200.0 psid pressure drop across the seal, the flowrate could be between 27.5 and 15.9 SCFM, which represents a difference of 42.2 percent.

In determining how the flow rate is affected by error in the clearance measurement, predictions were made for the baseline clearance ±2 percent. These predictions are shown in figure 12. Compared to thermal effects or machining tolerances, the range of flow rates is bounded much more closely, with a maximum variance of only 1.75 SCFM.

COMPARISON BETWEEN PREDICTED AND MEASURED FLOW RATES

Flow rates were predicted for the 50-mm Rayleigh-step, helium-purge seal by using clearance, eccentricity, and pressure measurements made during testing as input to the analysis. The inlet temperature was assumed to be 70 °F. These predicted flow rates are plotted against the measured flow rates in figure 13. If predictions and measurements were in complete agreement, the data should produce a straight line with a slope of 1.0 that passes through the origin. Obviously, this is not the case. The measured flow rates are approximately three to seven times greater than predicted, and the data follows the curve of a second-degree polynomial. This large discrepancy forces one to question the validity of the analytical model for this application. To verify that the analysis does accurately predict the gas flow rate through an annular seal with an axial pressure gradient, data independent of this experiment was sought.

Figure 14 shows data taken by Oike (ref. 3) with analytical predictions superimposed. A discharge coefficient of 0.6 was used. Agreement between the analysis and this data is very good. Also, data published by Nelson (ref. 4) show similar agreement. (See fig. 15.) In this case, discharge coefficients of 1.0 and 0.8 were used in predicting flow rates. To determine the reasonableness of using the selected discharge coefficients, predictions of the coefficients were made by using theoretical and empirical equations for annular orifices (ref. 5). For the configuration of Oike's work (ref. 3), the discharge coefficient is predicted to be between 0.68 and 0.55, depending on if the orfice is sharp-edged or square-edge and thick, respectively. The discharge coeffficient of choice, 0.6, falls in this range. For the configuration used in Nelson's (ref. 4) work, the discharge coefficient is predicted to be between 0.67 and 0.71, which is lower than what is needed to match the experimental data in figure 15. This discrepancy may be due to the longer length of the seal and the dominance of the equation for the film region over the flow nozzle equation for the inlet. It is interesting to note that the flows are choked for these two cases (refs. 3 and 4). Flow was not choked in the 50-mm Rayleigh-step, helium-purge, seal tests.

In considering the possible explanations for the discrepancy between the predicted and measured flow rates for the 50-mm Rayleigh-step, helium-purge seal several possibilities come to mind.

First, the unchoked flow portion of the analysis could be ignoring phenomena that significantly affect the flow rate, although the assumptions, equations, and trends found in parametric studies are reasonable. Unfortunately, no experimental data for unchoked flow through an annular clearance was found so that the analysis could be completely verified at this time. It is apparent, however, that the analysis does accurately predict flow rates for choked flow. This may be because the flow nozzle equation at the inlet dominates the film region equation when the flow is choked, which makes the flow rate less sensitive to the clearance measurement.

Second, there could be errors in the experimental data. Error in the measured clearance is one parameter that would have significant effects because flow rate is a function of the clearance cubed. The smallest possible clearance would occur if the shaft and seal ring were at ambient temperature and at maximum speed. The largest clearance would occur if the shaft temperature was that of liquid nitrogen and the seal ring remained at ambient temperature. Although it is not probable that these exact conditions did occur, they do provide a range within which the measured clearances should be. All the clearance measurements were between these two extremes of 0.00018 to 0.002934 in.

A third possible explanation for the discrepancy between measured and predicted flow rates may be that a second flow path existed between the housing and the seal ring. This could be due to imperfections in either the seal or the housing surface or both. Also, the carbon seal ring could be exhibiting an unstable geometry; twisting when exposed to cryogenic temperatures and large thermal gradients. In addition, MTI observed an inboard seal ring that developed an elliptical orbit in phase with the shaft orbit. They speculated that the frictional resistance of the seal ring was minimized by the existence of a fluid film between the ring and the end wall (ref. 2).

CONCLUDING REMARKS

Having no data to verify the unchoked flow analysis, and knowing there is the possibility of a secondary flow path and that small errors in the clearance measurement have great effect on the predicted unchoked flow rate, I recommend further testing be done. In addition to closely checking clearance and flow rate measurements, this testing should entail inspection of the axial lip and housing sealing surfaces for imperfections. Testing should be done at both room and cryogenic temperatures while particularly looking for twisting of the carbon seal at low temperatures. Also, a static test of the 50-mm, helium-purge seal and the seal runner configured in an apparatus that insures no secondary leakage at the axial lip should be conducted. Flow rates and clearances for several axial pressure gradients should be measured. If flow rates of this configuration were significantly less than those previously measured, I would conclude a secondary flow path did exist in previous testing. Comparisons of predicted and static test flow rates should then be made to verify the code. It is important to measure flow rates for both choked and unchoked flow to completely verify the analysis. By following these steps, the cause of the discrepancy between the analysis and measured data should be revealed.

SUMMARY OF RESULTS

Analytical data showed that the gas flow rate through an annular clearance with an axial pressure gradient increased with increased pressure drop across the seal. Flow rate also increased with higher downstream pressure because the density is higher; flowrate is greater for adiabatic flow than for isothermal flow. Flow rates decreased with elevated inlet temperature because of lower density and higher viscosity. Also, predictions found flow rates increased with eccentricity ratio, which is consistent with previous research. Study of those things that affect the radial clearance, such as centrifugal growth, thermal growth, machining tolerances, and clearance measurement uncertainty, placed wide boundaries on the expected flow rates. The widest boundaries were

due to thermal growth effects. Predicted flow rates underestimated measured flow rates for a 50-mm Rayleigh-step, helium-purge seal by three to seven times. However, the analysis accurately predicted the flow rates measured and reported by Oike, et al. and Nelson, et al. for choked gas flow through annular seals. Further testing is recommended.

TABLE I. - BASELINE INPUT FOR PREDICTED FLOWRATES THROUGH THE 50-mm RAYLEIGH-STEP, ANNULAR SHAFT SEAL

[Isothermal flow]

Downstream pressure, psia	14.7
Upstream temperature, °F	70.0
Seal length, in.	0.077
Shaft diameter, in.	1.9684
Radial clearance, in.	0.000669
Eccentricity ratio	0.0
Discharge coefficient	1.0
Viscosity, Reyns	2.8855×10^{-9}
Ratio of specific heats	1.66
Molecular weight	4.003

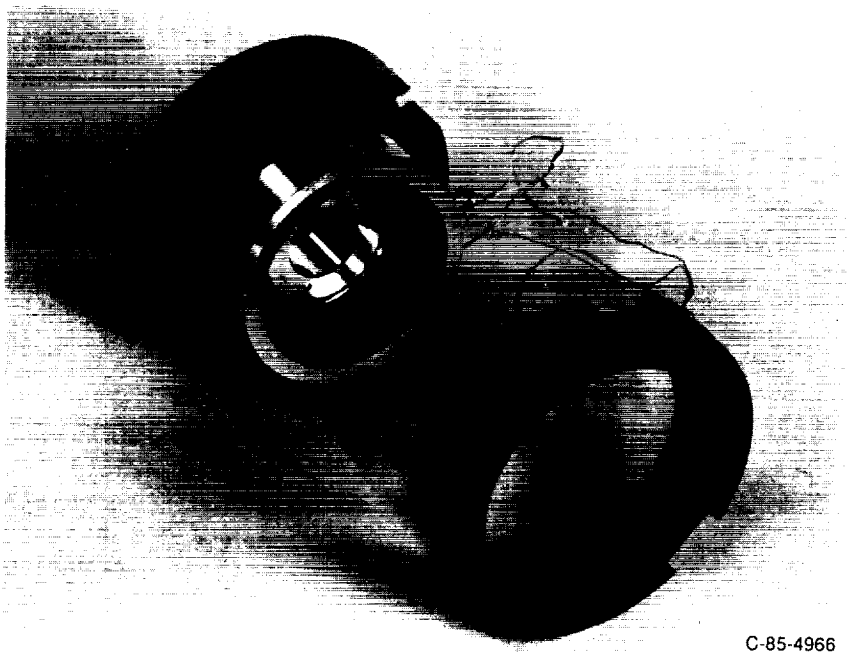

C-85-4966

Figure 1. - Rayleigh-step helium-purge annular seal pair with 50-mm runner. Ring is made of Purebon P5N carbon graphite and runner is Inconel 718.

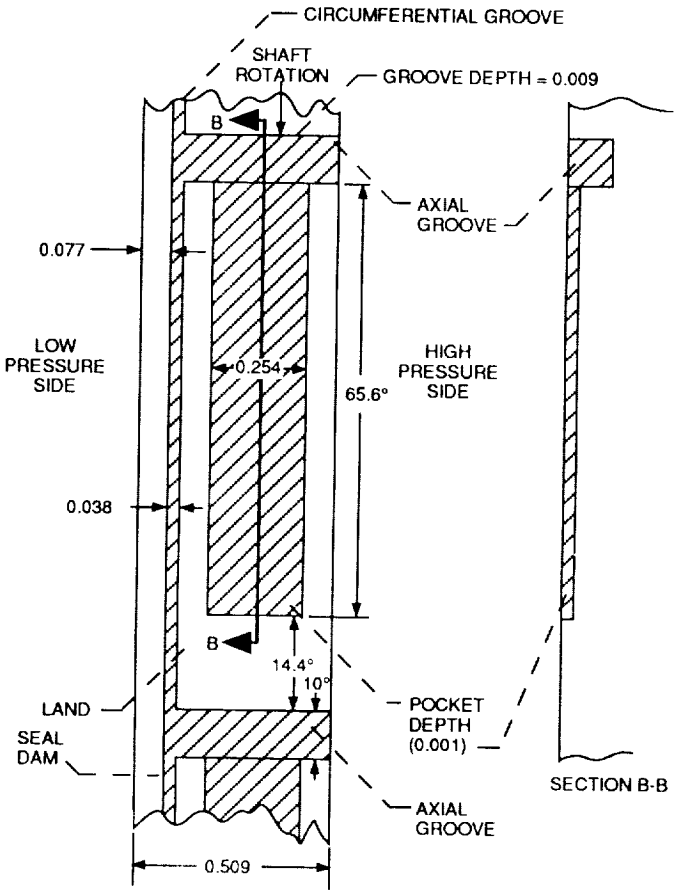

Figure 2. - Inner surface of the 50-mm Rayleigh-step, annular seal ring. (All linear dimensions are in inches.) Inside and outside seal ring diameters are 1.9694, and 2.66 inches, respectively.

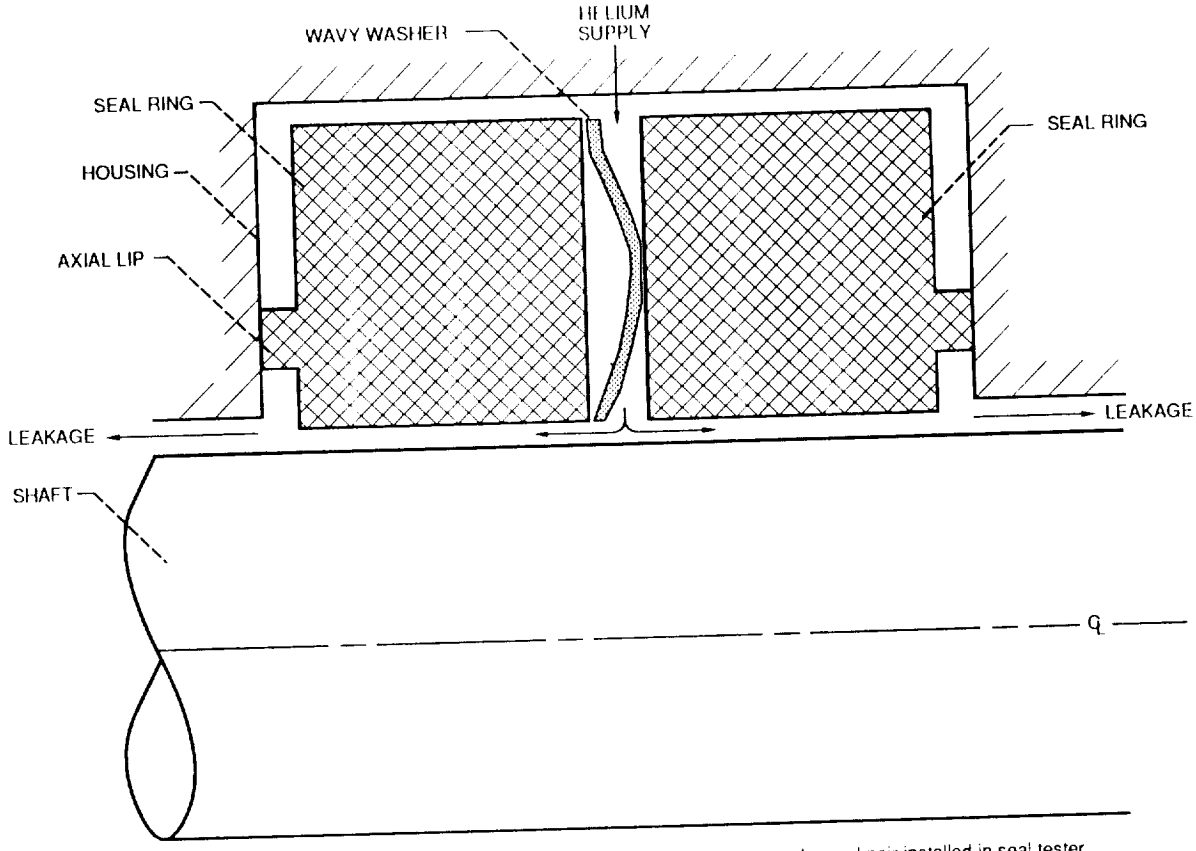

Figure 3. - Schematic of 50-mm Rayleigh-step, helium-purge, annular seal pair installed in seal tester.

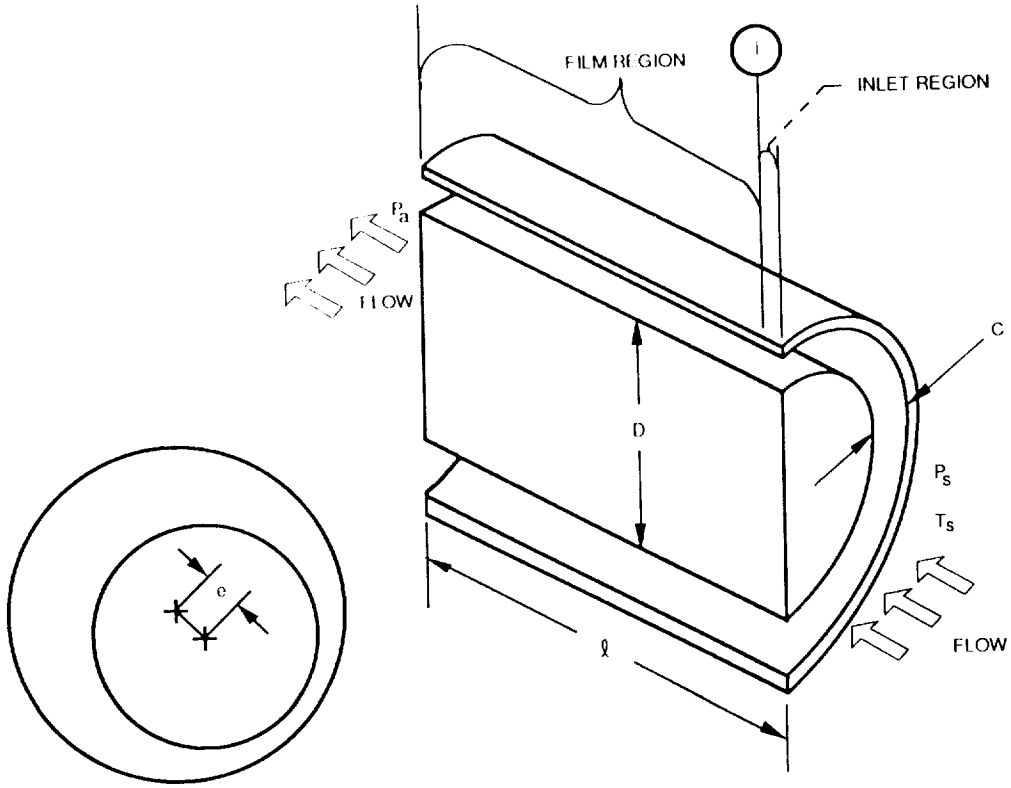

Figure 4. - Analytical Model of annular seal (with axial pressure gradient) used in FLOWCAL. D = shaft diameter, C = concentric radial clearance, ℓ = seal diameter length, e = eccentricity, ∈ = e/C (eccentricity ratio), and i = intermediate.

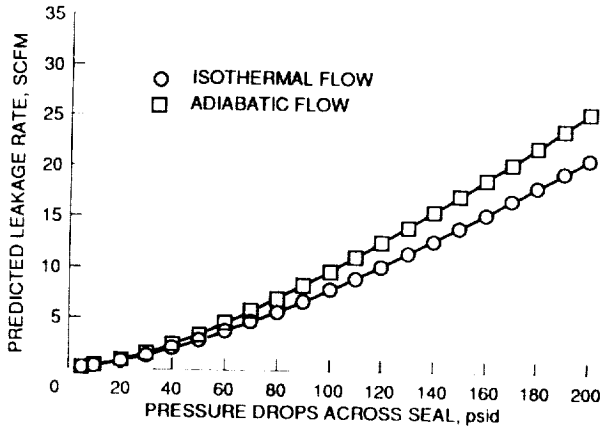

Figure 5. - Effect of isothermal and adiabatic flow on predicted leakage rate as a function of pressure frop across the 50-mm Rayleigh-step, helium purge, annular seal.

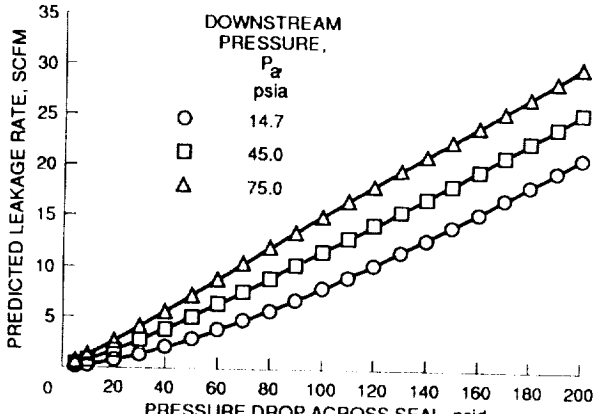

Figure 6. - Effect of downstream pressure on predicted leakage rate as a function of pressure drop across the 50-mm Rayleigh-step, helium purge, annular seal.

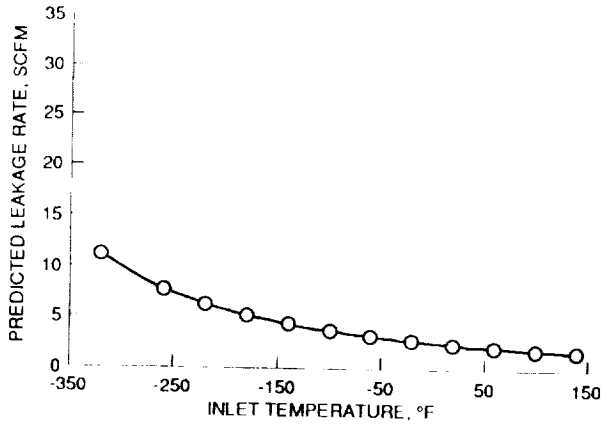

Figure 7. - Effect of inlet stream temperature on predicted leakage rate of 50-mm Rayleigh-step, helium purge, annular seal for pressure drop of 40.0 psid across seal.

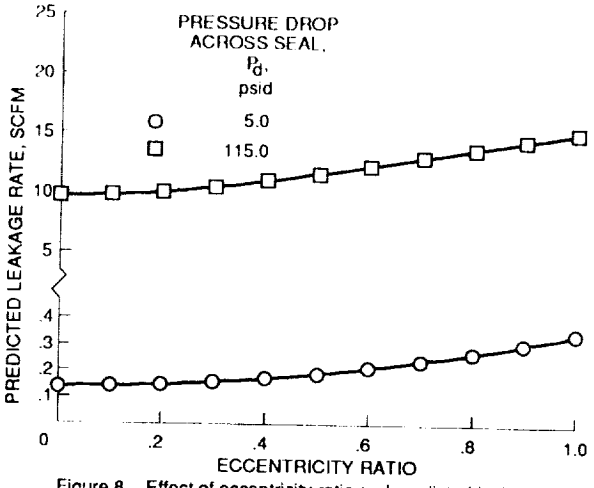

Figure 8. - Effect of eccentricity ratio and predicted leakage rate of 50-mm Rayleigh-step, helium-purge, annular seal for pressure drops across seal of 5.0 and 115.0 psid.

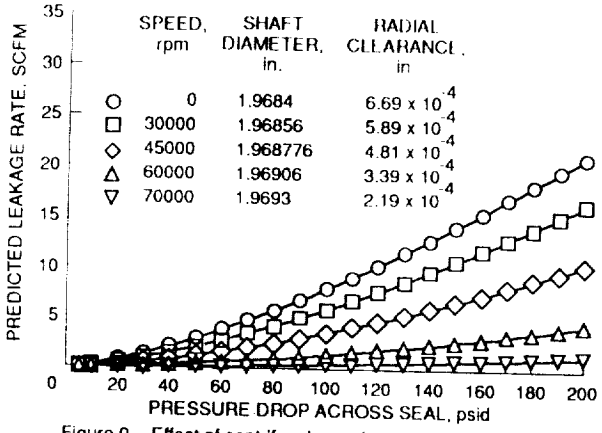

Figure 9. - Effect of centrifugal growth caused by shaft speed on predicted leakage rate as a function of pressure drop across the 50-mm Rayleigh-step, helium purge, annular seal.

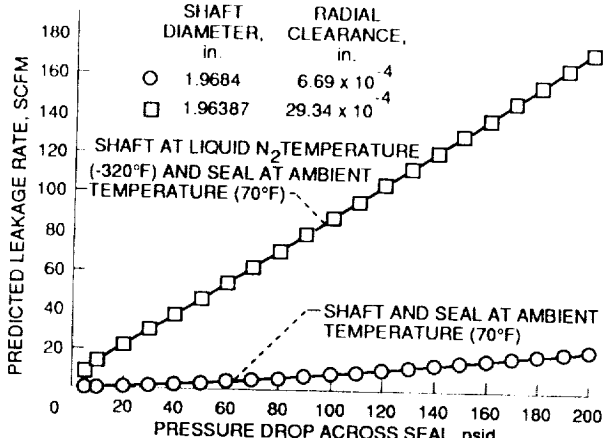

Figure 10. - Maximum and minimum predicted leakage rates caused by thermal growth changing the clearance of the 50-mm Rayleigh-step, helium purge, annular seal.

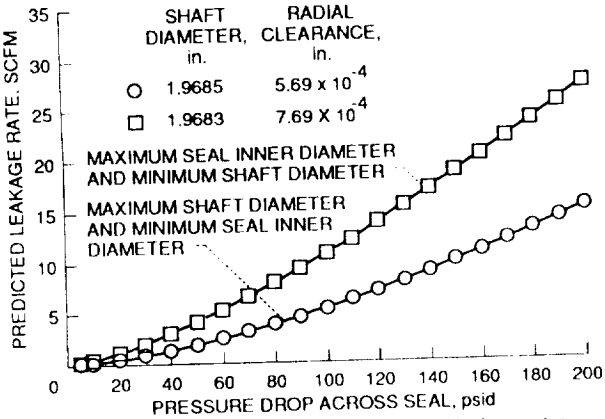

Figure 11. - Maximum and minimum predicted leakage rates caused by machining tolerances for 50-mm Rayleigh-step, helium-purge, annular seal.

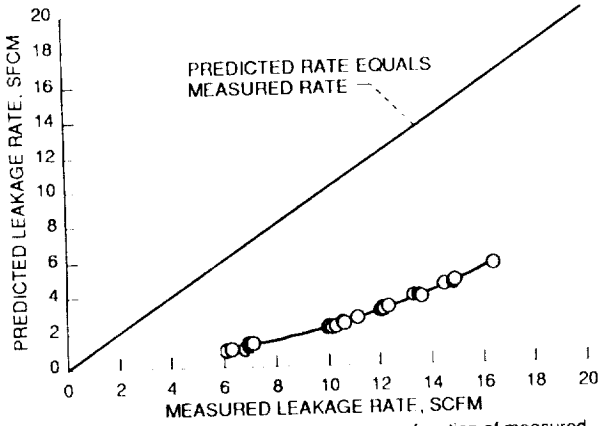

Figure 13. - Predicted leakage rates as a function of measured leakage rates for 50-mm Rayleigh-step, helium-purge, annular seal, compared to perfect prediction line.

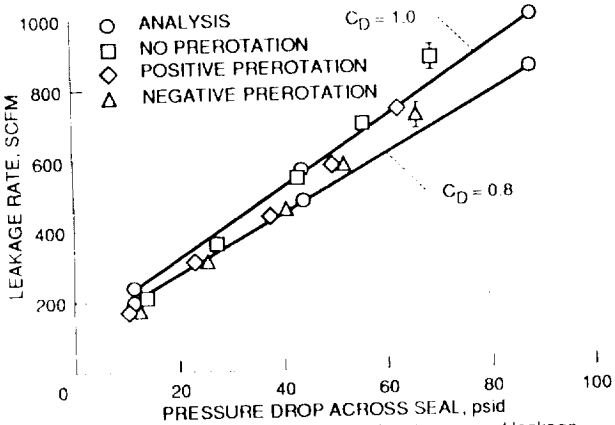

Figure 15. - Comparison of predicted and measured leakage rates for seal tested at Texas A&M University (ref. 4). Inlet temperature = 70 °F, downstream pressure = 14.7 psia, viscosity = 2.755 x 10^{-9} Reyns, specific heat ratio = 1.4, molecular weight = 28.9, seal length = 2.0 in., shaft diam = 6.0 in., radial clearance = 0.029 in., eccentricity ratio = 0.0, isothermal flow. Positive prerotation means the inlet flow had a circumferential velocity in the direction of shaft rotation. Negative prerotation is against the direction of shaft rotation.

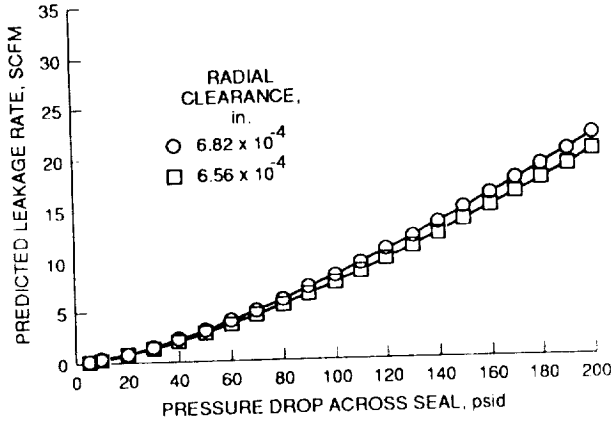

Figure 12. - Effect of a ±2 percent uncertainty in clearance measurement on predicted leakage rate for 50-mm Rayleigh-step, helium-purge, annular seal.

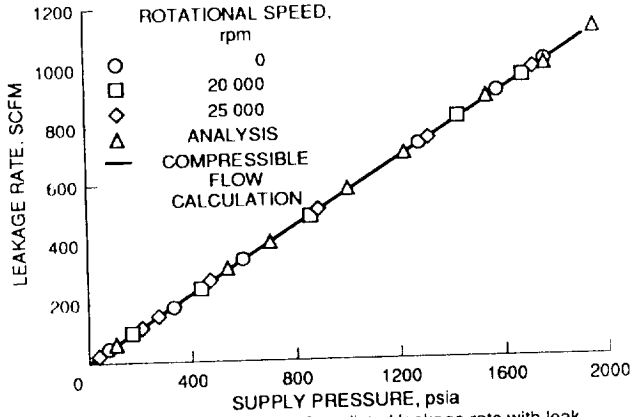

Figure 14. - Comparison of predicted leakage rate with leakage rate measured by Oike et al (ref. 3) for a Rayleigh-step, gaseous-hydrogen, annular seal. Inlet temperature = 95 °F, downstream pressure = 14.7 psia, viscosity = 0.121 x 10^{-8} Reyns, specific heat ratio = 1.39, seal length = 0.28 in., shaft diam. = 1.97 in., radial clearance = 2.26 x 10^{-3} in., eccentricity ratio = 0.0, discharge coefficient = 0.6, molecular weight = 2.0, adiabatic flow.

APPENDIX - FLOW RATE PREDICTIONS FOR 20-mm RAYLEIGH-STEP, HELIUM-PURGE, ANNULAR SEAL

TABLE II. - BASELINE INPUT FOR PREDICTION OF FLOW RATES THROUGH THE 20-mm DIAMETER, RAYLEIGH-STEP, ANNULAR SHAFT SEAL

[Isothermal flow]

Downstream pressure, psia	14.7
Upstream temperature, °F	70.0
Seal length, in.	0.077
Shaft diameter, in.	0.78745
Radial clearance, in.	0.000325
Eccentricity ratio	0.0
Discharge coefficient	1.0
Viscosity, Reyns	2.8855x10-9
Ratio of specific heats	1.66
Molecular weight	4.003

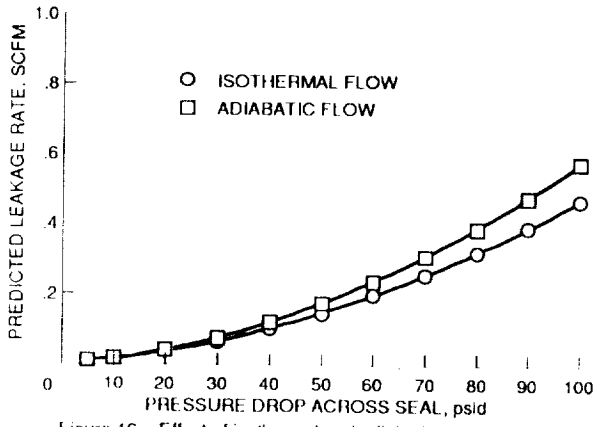

Figure 16. Effect of isothermal and adiabatic flow on predicted leakage rate as a function of pressure drop across the 20-mm Rayleigh-step, helium-purge, annular seal.

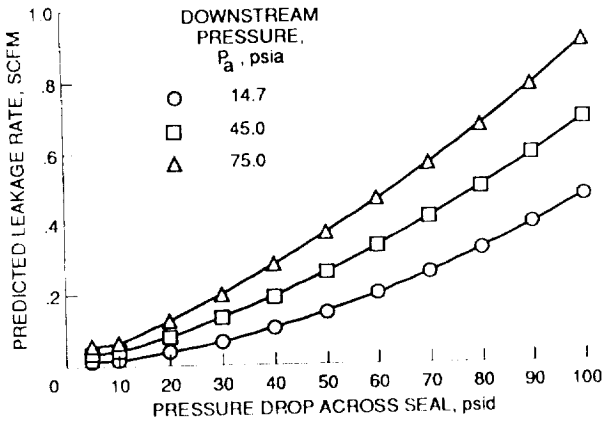

Figure 17. - Effect of downstream pressure on predicted leakage rate as a function of pressure drop across 20-mm Rayleigh-step, helium-purge, annular seal.

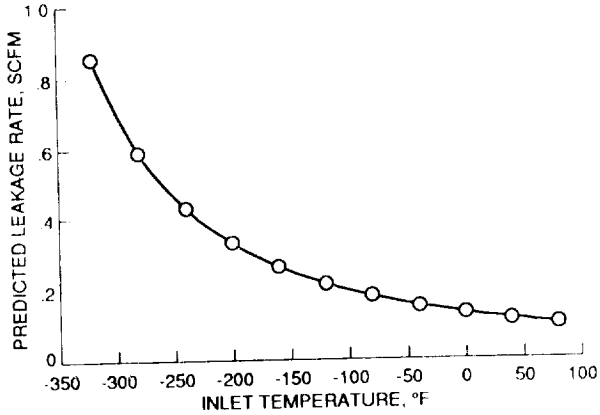

Figure 18. - Effect of inlet stream temperature on predicted leakage rate of 20-mm Rayleigh-step, helium-purge, annular seal with a pressure drop across the seal of 40.0 psid.

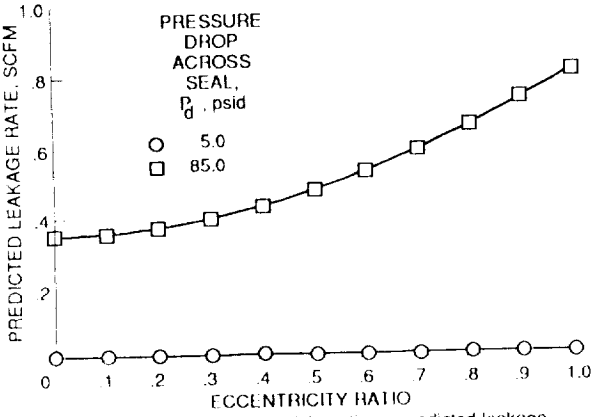

Figure 19. - Effect of eccentricity ratio on predicted leakage rate of 20-mm Rayleigh-step, helium-purge, annular seal for pressure drops across seal of 5.0 and 85.0 psid.

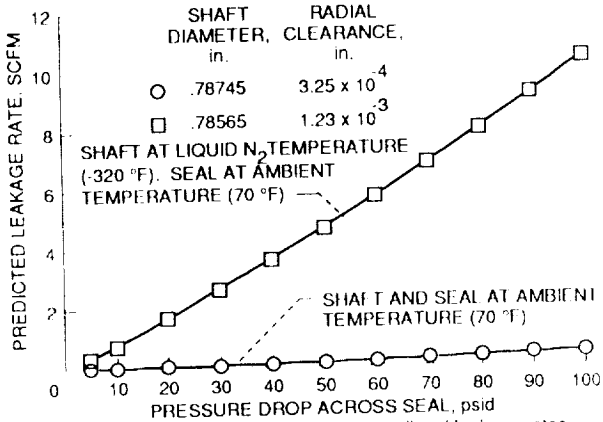

Figure 20. - Maximum and minimum predicted leakage rates caused by thermal growth changing the clearance in the 20 mm Rayleigh-step, helium-purge, annular seal.

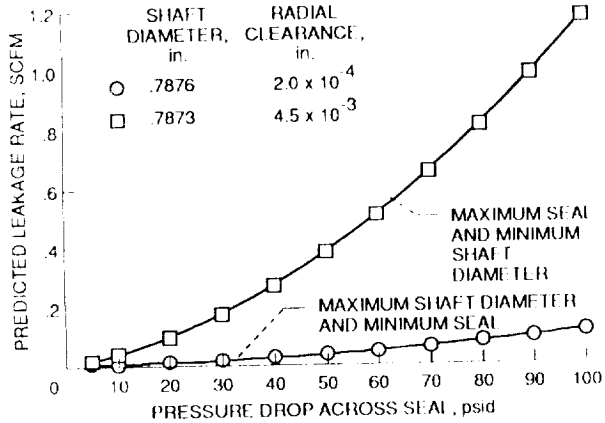

Figure 21. - Maximum and minimum predicted leakage rates due to machining tolerances for 20 mm Rayleigh-step, helium-purge, annular seal.

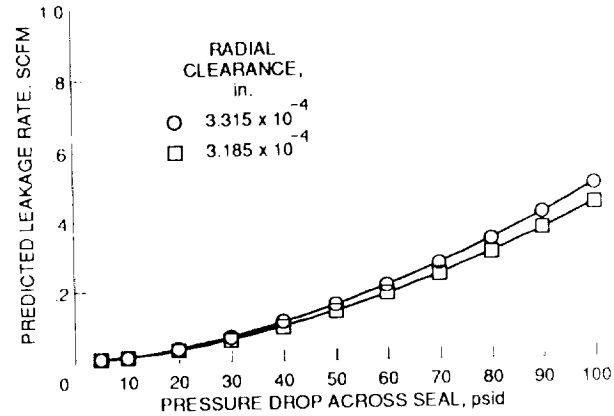

Figure 22. - Effect of ±2 percent uncertainty in clearance measurements on predicted leakage rates for 20-mm Rayleigh-step, helium-purge, annular seal

REFERENCES

1. Tao, L.N.; and Donovan, W.F.: Through-Flow in Concentric and Eccentric Annuli of Fine Clearance With and Without Relative Motion of the Boundaries. ASME Trans., vol. 77, no. 7, Nov. 1955, pp. 1291-1301.

2. Shapiro, W.; and Hamm, R.: Seal Technology for Liquid Oxygen (LOX) Turbopumps. (REPT-85TR20, Mechanical Technology Inc.; NASA Contract NAS3-23260) NASA CR-174866, 1985.

3. Oike, M., et al.: Experimental Study on High-Pressure Gas Seals for LOX Turbopumps. 15th International Symposium on Space Technology and Science, Vol. 1, H. Matsuo, ed., AGNE Publishing Inc., Tokyo, Japan, 1986, pp. 365-374.

4. Nelson, C.C., et al.: Theory Versus Experiment for the Rotordynamic Coefficients of Annular Gas Seals: Part 2 - Constant-Clearance and Convergent-Tapered Geometry. ASME Paper 85-Trib-2, Mar. 1985.

5. Bell, K.J.; and Bergelin, O.P.: Flow Through Annular Orifices. ASME Trans., vol. 79, no. 3, Apr. 1957, pp. 593-601.

NASA
National Aeronautics and Space Administration

Report Documentation Page

1. Report No.	2. Government Accession No.	3. Recipient's Catalog No.
NASA TM-101352		

4. Title and Subtitle	5. Report Date
Leakage Predictions for Rayleigh-Step, Helium-Purge Seals	December 1988
	6. Performing Organization Code

7. Author(s)	8. Performing Organization Report No.
Margaret P. Proctor	E-4379
	10. Work Unit No. 506-42-21

9. Performing Organization Name and Address	11. Contract or Grant No.
National Aeronautics and Space Administration Lewis Research Center Cleveland, Ohio 44135-3191	13. Type of Report and Period Covered Technical Memorandum

12. Sponsoring Agency Name and Address	14. Sponsoring Agency Code
National Aeronautics and Space Administration Washington, D.C. 20546-0001	

15. Supplementary Notes

16. Abstract

Rayleigh-step, helium-purge, annular shaft seals, studied for use in liquid oxygen turbopumps, generate a hydrodynamic force that enables the seal to follow shaft perturbations. Hence, smaller clearances can be used to reduce the seal leakage. FLOWCAL, a computer code developed by Mechanical Technology Incorporated, predicts gas flow rate through an annular seal with an axial pressure gradient. Analysis of a 50-mm Rayleigh-step, helium-purge, annular seal showed the flow rate increased with increased axial pressure gradient, downstream pressure, and eccentricity ratio. Increased inlet temperature reduced the leakage. Predictions made at maximum and minimum clearances (due to centrifugal and thermal growths, machining tolerances and ±2 percent uncertainty in the clearance measurement) placed wide boundaries on expected flow rates. The widest boundaries were set by thermal growth conditions. Predicted flow rates for a 50-mm Rayleigh-step, helium-purge, annular seal underestimated measured flow rates by three to seven times. However, the analysis did accurately predict flow rates for choked gas flow through annular seals when compared to flow rates measured in two other independent studies. Possible causes for the discrepancy found between measured and predicted flow rates are discussed. Further testing is recommended.

17. Key Words (Suggested by Author(s))	18. Distribution Statement
Seal; Rayleigh; Rayleigh-step; Helium-purge; Leakage; Predictions; LOX-turbopump; Flow rate	Unclassified – Unlimited Subject Category 20

19. Security Classif. (of this report)	20. Security Classif. (of this page)	21. No of pages	22. Price*
Unclassified	Unclassified	18	A03

*For sale by the National Technical Information Service, Springfield, Virginia 22161

National Aeronautics and
Space Administration

Lewis Research Center
Cleveland, Ohio 44135

SECOND CLASS MAIL

ADDRESS CORRECTION REQUESTED

Official Business
Penalty for Private Use $300

Postage and Fees Paid
National Aeronautics and
Space Administration
NASA-451

NASA